Surface hopping, transition state theory and decoherence. I. Scattering theory and time-reversibility

Amber Jain, Michael F. Herman, Wenjun Ouyang, and Joseph E. Subotnik

Citation: The Journal of Chemical Physics **143**, 134106 (2015); doi: 10.1063/1.4930548
View online: http://dx.doi.org/10.1063/1.4930548
View Table of Contents: http://scitation.aip.org/content/aip/journal/jcp/143/13?ver=pdfcov
Published by the AIP Publishing

Surface hopping, transition state theory and decoherence. I. Scattering theory and time-reversibility

Amber Jain,[1] Michael F. Herman,[2] Wenjun Ouyang,[1] and Joseph E. Subotnik[1,a)]
[1]*Department of Chemistry, University of Pennsylvania, 231 South 34th Street, Philadelphia, Pennsylvania 19104, USA*
[2]*Department of Chemistry, Tulane University, New Orleans, Louisiana 70118, USA*

(Received 17 June 2015; accepted 24 August 2015; published online 2 October 2015)

We provide an in-depth investigation of transmission coefficients as computed using the augmented-fewest switches surface hopping algorithm in the low energy regime. Empirically, microscopic reversibility is shown to hold approximately. Furthermore, we show that, in some circumstances, including decoherence on top of surface hopping calculations can help *recover* (as opposed to destroy) oscillations in the transmission coefficient as a function of energy; these oscillations can be studied analytically with semiclassical scattering theory. Finally, in the spirit of transition state theory, we also show that transmission coefficients can be calculated rather accurately starting from the curve crossing point and running trajectories forwards and backwards. © *2015 AIP Publishing LLC.* [http://dx.doi.org/10.1063/1.4930548]

I. INTRODUCTION

The birth of the fewest switches surface hopping (FSSH) method in 1990 laid the frame-work for an efficient and powerful approach to perform semiclassical nonadiabatic dynamics.[1] While surface hopping was originally formulated to describe electronic transitions in the course of gas-surface scattering, in recent years, the method has been used often to describe a number of other processes such as photoexcited dynamics and proton transfer.[2–4] Many photo-excited experiments can be characterized by simulations of 1-50 ps, and these have now become standard with surface hopping dynamics.

Apart from photo-excited experiments, a separate class of experiments is rare events starting on the ground state. One can consider, e.g., the famous Fe^{+2}/Fe^{+3} electron transfer popularized by Marcus.[5] The time scale for thermal electron transfer can be as long as milliseconds (or even seconds), requiring extraordinarily long trajectories. For such processes, there is no alternative but to use some variant of transition state theory (TST) combined with dynamics near the top of the barrier to capture all the electronic, nonadiabatic dynamical effects.[6–10] In Paper II,[11] we will discuss and implement an algorithm for computing thermal rate constants based on a variant of the Hammes-Schiffer and Tully (HST) approach.[12]

Before we investigate the details of any specific algorithm for thermal rate constants in the condensed phase, however, the goal of the present article is to examine some conceptual issues in the gas phase facing all surface hopping algorithms. These issues are as follows.

1. Formally, surface hopping is not time-reversible.[13] Thus, unlike the case of classical dynamics, one is not guaranteed that forward and backward rate constants will obey detailed balance. Thus, even if we could run very long surface hopping trajectories, there is no guarantee that our rate constants would satisfy a central tenet of rate theory.

2. Even if the surface hopping trajectories were time-reversible, it is unclear how to initialize surface hopping trajectories at the transition state (TS) for a rare event crossing — because of the lack of the knowledge of the quantum amplitudes ("c_j") discussed below. This lack of a simple initialization protocol is a significant drawback to the surface hopping protocol (and was the inspiration for the HST algorithm).

3. The third and the final complication is that recent studies have shown without doubt that a decoherence correction is necessary to achieve correct long time dynamics using surface hopping dynamics.[14–19] Decoherence corrections can be expected to increase the time irreversibility of a surface hopping trajectory and, therefore, the implications of a decoherence correction on detailed balance must be examined.

The goals of this paper are to address these three issues for a simple one-dimensional scattering problem in the gas phase, where some analytic results can help the interpretation.[20–23] In Paper II, we will address these same issues in the confines of rate theory and the Marcus problem (which we consider a one-dimensional problem with friction).[24] In this paper, our approach will be as follows.

1. Detailed balance can be viewed as a consequence of the time-reversal symmetry for a fixed total energy E: the transmission factor $\kappa(E)$ should be identical going from left to right and right to left. We will investigate the symmetry of the transmission factors from a surface hopping algorithm. We will find that these transmission factors are roughly equal in practice; some analytic results will be derived to predict how different these transmission factors can be. Overall, our conclusions based on the symmetry of the transmission factors will be in line with those of Schmidt, Parandekar, and Tully,[25] as well as Sherman and Corcelli,[26] who have shown that surface hopping approximately yields the correct equilibrium Boltzmann populations for long simulations.

a)Electronic mail: subotnik@sas.upenn.edu

2. Regarding the initialization of trajectories at the crossing point, in this paper, we will use an approximation of the HST scheme, whereby we run surface hopping dynamics only in the forward direction (and adiabatic dynamics in the backwards direction). We will check numerically (in Sec. V D) as to the robustness of our approach, i.e., how sensitive are we to the choice of the dividing surface?

3. As for decoherence, in this paper we will present results using standard surface hopping (FSSH) and our own decoherence-corrected A-FSSH algorithm. Already in the literature, we have shown that A-FSSH correctly recovers Marcus theory and Redfield theory (in the high temperature limit where the nuclei can be considered classical).[18,19] Here, we will investigate whether and how including collapsing events alter the symmetry of the transmission factor T(E) (and thus whether and how decoherence affects detailed balance). Empirically, we will find that including decoherence always improves results without harming detailed balance.

Before we present our methods and results, we note that several other methods exist in literature to compute the transmission factor. The most well-known theory is the Landau-Zener (LZ) formalism that computes the probability of diabatic transitions for a one-dimensional scattering problem.[27,28] The work of Zhu and Nakamura (ZN) significantly improved the accuracy of the LZ formalism, and ZN results were shown to be applicable across a wide range of energies.[29,30] A surface hopping scheme based on this ZN formalism was later developed, giving highly promising results.[31–33] In a different approach, recently Jasper computed transmission factors for weakly coupled systems using short-time trajectories. Significantly, Jasper has demonstrated the importance of multidimensional effects, particularly the variance of transmission probability with the energy in the orthogonal modes.[34]

An outline of the paper is as follows: In Sec. II, our one dimensional model Hamiltonian is described. Section III describes the computation of transmission coefficient either directly or using a TST approach. This section also provides a derivation of the analytical (semiclassical) theory to compute transmission coefficients. Computational details for the A-FSSH calculations and exact quantum mechanical calculations are given in Sec. IV, and results are provided in Sec. V. The conclusions of the paper are given in Sec. VI.

II. MODEL HAMILTONIAN

For the purposes of this paper, we will study a variation of Tully's simple avoided crossing model (model problem #1). The potentials in the diabatic representation are given by

$$V_{11}(x) = A\tanh(B_1 x), \tag{1}$$

$$V_{22}(x) = -A\tanh(B_2 x) - \epsilon, \tag{2}$$

$$V_{12}(x) = V_{21}(x) = C\exp\left(-Dx^2\right). \tag{3}$$

The parameters are chosen to be $A = 0.03$, $B_1 = 1.6$, $B_2 = 2.4$ (or 1.6), $C = 0.0005$ (or 0.005), $D = 1$, and $\epsilon = 0.007$, all in atomic units. The mass (m) is 2000 a.u. Note that we choose two different values of B because, as will be shown below, the case $B_1 = B_2$ is a special case where accurate semiclassical dynamics are surreptitiously easy to recover. The two values of C have been chosen so that the model Hamiltonian should sit either in the diabatic or the adiabatic regimes, respectively. The adiabatic potential energy surfaces corresponding to $B_2 = 2.4$ and $C = 0.0005$ are shown in Fig. 1. We work exclusively in the low energy regime ($E < 0.02$ a.u.) where both upper channels are not accessible asymptotically.

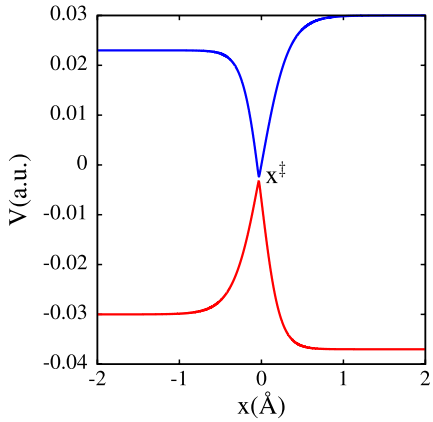

FIG. 1. The adiabatic surfaces with $B_2 = 2.4$ and $C = 0.0005$. $x^{\ddagger}$ is the diabatic curve crossing point.

III. METHODS

In this paper, we will study two different approaches for calculating transmission coefficients: (i) a direct scattering approach and (ii) a transition state approach.

A. Direct computation with A-FSSH dynamics

The most direct method to compute the transmission coefficients is to initiate a set of trajectories to the left of the curve crossing at $x = -2$ Å (see Fig. 1). These trajectories are then evolved using A-FSSH dynamics with positive velocity and terminated when $|x| > 2$ Å. For the energy regimes studied in this paper, the upper transmission channel is always closed. Thus, every trajectory that reaches the right hand side must switch diabats; alternatively, the trajectory must return back to the left side. The transmission coefficient can then be computed as the fraction of the trajectories that are terminated on the right side. For completeness, we have recapitulated the basic steps of an A-FSSH calculation[18] in Appendix A. The only differences between the current paper and Ref. 18 are (i) a slightly simplified treatment of the moments adjustment after a hop and (ii) the occasional reversal of velocity on encountering frustrated hops.[35]

B. Transition state formalism

The above method can be computationally expensive in the presence of a large barrier if there is moderate to strong friction. With this in mind and in the context of transition state theory, we would like to evaluate the transmission coefficients from trajectories starting at the crossing point $x^{\ddagger}$ (see Fig. 1).

For the sake of simplicity, in this article, we will use a simple approximation of the Hammes-Schiffer and Tully scheme:[12,36] 1. We run trajectories backwards in time from the dividing surface to figure out the necessary quantum

amplitudes c_j [in Eq. (A3)]. We will run these backward trajectories entirely along the ground adiabatic surface. In making this approximation, we assume that the important nonadiabatic effects occur near the curve crossing and can be recovered by a relatively short trajectory on one surface. We ignore multiple crossing events that would lead to complicated pattern.[37] 2. Next, we run trajectories forward in time from the dividing surface using the A-FSSH algorithm, where hops are now allowed. Note that, without the first step of this protocol going backwards (i.e., without a set of c_j's), the A-FSSH algorithm cannot decide when or where to hop.

Admittedly, the protocol just invoked might seem unnatural and even incorrect to the reader. After all, one might argue that the scheme grossly breaks time-reversibility: the backwards propagation is treated at a different level of theory than forward propagation. That being said, it is important to remember that direct FSSH itself is not time-reversible. A fully time-reversible FSSH algorithm requires negative weighting that is not stable numerically.[13,38] In practice, one of the goals of this paper is to check whether this approximate TST scheme and/or direct FSSH dynamics recover equal transmission coefficients going forwards (left to right) or backwards (right to left), as required by time reversibility.

In summary, the algorithm is as follows.

1. Initialize the position $x = x^{\ddagger}$, and the momentum $P = -\sqrt{2m(E - V_1(x^{\ddagger}))}$. To compute the necessary quantum amplitudes, set[12]

$$\mathbf{U}(0) = \begin{pmatrix} 1 & 0 \\ 0 & 1 \end{pmatrix}. \tag{4}$$

2. For a time step dt, back-evolve
   - the classical dynamics using

$$\dot{x} = \frac{P}{m}, \tag{5}$$

$$\dot{P} = -\frac{\partial V_1}{\partial x}, \tag{6}$$

   - the quantum dynamics using

$$i\hbar\dot{\mathbf{U}} = -\begin{pmatrix} V_1 & -i\hbar(P/m)d_{12} \\ i\hbar(P/m)d_{12} & V_2 \end{pmatrix}\mathbf{U}. \tag{7}$$

   Backwards evolve for a time interval t_R until $x < -2$ Å is satisfied.
3. Now return to the crossing point ($x = x^{\ddagger}$). Set $P = \sqrt{2m(E - V_1(x^{\ddagger}))}$ and initialize all the moments to be 0. The quantum amplitudes are initiated by

$$c_j(0) = U^{\dagger}_{j1}(t_R). \tag{8}$$

   The ansatz in Eq. (8) is equivalent to initializing with $(c_1, c_2) = (1, 0)$ at $x = -2$ Å and forward evolution (on the ground surface) until $x = x^{\ddagger}$.
4. Choose a random number $\zeta \in [0, 1]$. If $\zeta < |c_1(0)|^2$, set the initial surface as $i = 1$. Otherwise, set $i = 2$ and adjust the momentum to conserve energy [see Eq. (A9)]. If the upper adiabat is energetically inaccessible (i.e., the momentum adjustment leads to complex velocity) the trajectories are initiated on the ground surface.
5. Forward evolve with steps (2-5) of regular A-FSSH algorithm described in Appendix A until $|x| > 2$ Å is satisfied. The transmission coefficient, similar to the direct computation, is computed as the fraction of trajectories that terminate with $x > 2$ Å.

We re-emphasize that our scheme is not new. In the context of transition state theory (and kinetic rates), Hammes-Schiffer and Tully[12] (HST) long ago suggested running a swarm of quasi-stochastic trajectories backwards with an approximate hopping criteria that is independent of the quantum amplitudes, and then later correcting for these approximate hopping probabilities by appropriate weightings. In principle, with enough trajectories and reweightings, the HST approach should recover precisely the results of direct dynamics and be invariant to the choice of the dividing surface.

C. Semiclassical, analytical treatment of the diabatic regime

Numerical studies of direct A-FSSH dynamics and TS dynamics are usually all that is possible when benchmarking surface hopping results.[18,39,40] That being said, in the diabatic limit of a one-dimensional problem, a semiclassical theory of A-FSSH transmission coefficients can be derived. This analytical theory can help us understand both (i) the time-reversible successes/failures of surface hopping dynamics and (ii) the implications of including/not including decoherence in our transmission coefficients.

The transmission coefficient can be computed as the result of three crossings as shown in Fig. 2. A general semiclassical analysis for multiple recrossings has been performed by

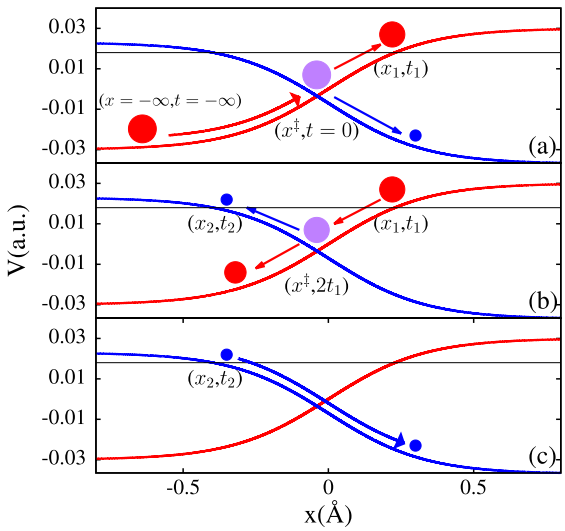

FIG. 2. A schematic view of transmission from diabat 1 (red) to diabat 2 (blue) shown in 3 steps. (a) In the first crossing of diabats, P_{LZ} fraction of trajectories get transmitted (blue arrow) and the remaining trajectories continue on diabat 1 (red arrow). (b) The trajectories that continue on diabat 1 turn around after reaching the classical turning point x_1 and recross the dividing surface, again with some trajectories switching diabats (blue arrow) (c) Those trajectories that switched to diabat 2 in step (b) reverse their velocities at x_2 and are all transmitted as shown by the blue arrow. This sequence assumes that decoherence occurs near x_2 and ignores events with probability P^2_{LZ}. The total energy of the system is 0.015 a.u. (see the black line).

Herman long ago.[20–23] Drawing inspiration from these works, we compute the total transmission coefficient in the context of the A-FSSH algorithm. We consider the case where all upper channels are closed asymptotically and the particle can escape only on the lower adiabat. Numerical simulations for our model system suggest that the A-FSSH algorithm tends to collapse the amplitudes (i.e., promote a decoherence event) near x_2 (and almost always to the left of $x^\ddagger$) in Fig. 2(b). See Appendix C. While one can only speculate for now as to how general this conclusion about decoherence location is, this assumption works very well at-least for the Hamiltonian in Eqs. (1)-(3). With this in mind, the final result for the A-FSSH transmission coefficient (κ) can be shown to be

$$\kappa = \begin{cases} 4P_{LZ}\cos^2(\psi - \pi/4), & 4\cos^2(\psi - \pi/4) > 1 \\ P_{LZ}, & \text{otherwise} \end{cases}, \quad (9)$$

where

$$\psi = \frac{1}{\hbar}\int_0^{t_1} dt\left(V_1^d(t) - V_2^d(t)\right). \quad (10)$$

Here, $t = 0$ is the time corresponding to the trajectory sitting at the curve-crossing and t_1 corresponds to the time at which the trajectory reaches the turning point x_1 (see Fig. 2(a)); $V_{1/2}^d$ represents the diabatic potentials. The LZ probability of transmission (in the diabatic limit) is

$$P_{LZ} = \frac{2\pi V_c^2}{v_0 \hbar F_{12}}, \quad (11)$$

where V_c is the diabatic coupling (assumed to be independent of position), v_0 is the velocity, and F_{12} is the magnitude of the difference of the diabatic slopes at curve-crossing.

To derive Eq. (9), we consider the contribution to the transmission coefficient from each crossing shown in Fig. 2.

1. Crossing 1

Obviously, at the first pass through the crossing point, P_{LZ} fraction of trajectories get transmitted (see Fig. 2(a)). Before moving on to the next steps, we will need to calculate the diabatic coefficients (d_i) for the trajectories that continue on diabat 1 (shown by the red arrow in Fig. 2(a)) as the trajectory goes from $x = -\infty$ to $x = x_1$. To that end, we define A_1 and B_1 as[27,28]

$$A_1(t) = d_1(t)\exp\left[i/\hbar\int_0^t dt' V_1^d(t')\right], \quad (12)$$

$$B_1(t) = d_2(t)\exp\left[i/\hbar\int_0^t dt' V_2^d(t')\right], \quad (13)$$

with $t = 0$ defined to be the time when the trajectory reaches $x = x^\ddagger$. Substituting into the Schrödinger equation,

$$i\hbar\begin{pmatrix}\dot{d}_1\\ \dot{d}_2\end{pmatrix} = \begin{pmatrix}V_1^d & V_c\\ V_c & V_2^d\end{pmatrix}\begin{pmatrix}d_1\\ d_2\end{pmatrix}, \quad (14)$$

gives

$$i\hbar\dot{B}_1 = V_c A_1 \exp\left[i/\hbar\int_0^t dt'(V_2^d(t') - V_1^d(t'))\right]. \quad (15)$$

The initial conditions are given by $d_1 = 1$ and $d_2 = 0$. We solve this differential equation assuming A_1 does not change with time, and the LZ approximation

$$V_2^d - V_1^d = -v_0 F_{12} t, \quad (16)$$

where $v_0 > 0$ is the velocity at $t = 0$. This leads to

$$B_1(t_1) \simeq B_1(-\infty) - i/\hbar V_c A_1 \int_{-\infty}^{t_1} dt \exp\left[i/\hbar(-v_0 F_{12} t^2/2)\right], \quad (17)$$

$$A_1(t_1) \simeq A_1(-\infty). \quad (18)$$

Next, we assume that t_1 is large enough such that the $B_1(t_1) = B_1(\infty)$. This assumption is roughly valid since the phases accumulated on d_i will be dominated by the phases in Eq. (12). This gives (using $B_1(-\infty) = 0$)

$$B_1(t_1) \simeq A_1(-\infty)\sqrt{P_{LZ}}\exp\left[-3i\pi/4\right]. \quad (19)$$

The phase $-3i\pi/4$ in Eq. (19) can be easily derived by performing a contour integration.[28] Substituting Eqs. (18) and (19) in Eqs. (12) and (13), we get

$$d_1(t_1) = A_1(-\infty)\exp\left[-i/\hbar\int_0^{t_1} dt' V_1^d(t')\right], \quad (20)$$

$$d_2(t_1) = A_1(-\infty)\sqrt{P_{LZ}}\exp\left[-3i\pi/4\right] \times \exp\left[-i/\hbar\int_0^{t_1} dt' V_2^d(t')\right]. \quad (21)$$

2. Crossing 2

Now, we consider the second crossing event (Fig. 2(b)), where the trajectories on the upper surface reverse their motion. The trajectories that continue on diabat 1 through the crossing (shown by the red arrow in Fig. 2(b)) do not contribute to the transmission and are ignored. We must compute the fraction of trajectories that will hop to diabat 2 (the blue arrow in Fig. 2(b)), and their diabatic coefficients at x_2.

We follow the same steps as for the first crossing. Before defining A_2 and B_2 similar to Eq. (12), we note that in the absence of any friction, the trajectory will retrace itself from $x = x_1$ to $x = x^\ddagger$. Hence, the time when the trajectory reaches $x = x^\ddagger$ is $t = 2t_1$ with velocity $-v_0$. With this, we define

$$A_2(t) = d_1(t)\exp\left[i/\hbar\int_{2t_1}^t dt' V_1^d(t')\right], \quad (22)$$

$$B_2(t) = d_2(t)\exp\left[i/\hbar\int_{2t_1}^t dt' V_2^d(t')\right], \quad (23)$$

with

$$i\hbar\dot{B}_2 = V_c A_2 \exp\left[i/\hbar\int_{2t_1}^t dt'(V_2^d(t') - V_1^d(t'))\right]. \quad (24)$$

Originally, at time t_1, it is straightforward to show that

$$A_2(t_1) = d_1(t_1)\exp\left[i/\hbar\int_{2t_1}^{t_1} dt' V_1^d(t')\right] \quad (25)$$

$$= A_1(-\infty)\exp\left[-2i/\hbar\int_0^{t_1} dt' V_1^d(t')\right], \quad (26)$$

$$B_2(t_1) = d_2(t_1)\exp\left[i/\hbar\int_{2t_1}^{t_1} dt' V_2^d(t')\right] \quad (27)$$

$$= A_1(-\infty)\sqrt{P_{LZ}}\exp\left[-3i\pi/4\right] \times \exp\left[-2i/\hbar\int_0^{t_1} dt' V_2^d(t')\right]. \quad (28)$$

In Eqs. (26) and (28), we have plugged in Eqs. (20) and (21). Also, we have used time reversibility (as was mentioned above); the trajectory retraces itself exactly from time t_1 to $2t_1$, compared to the forward evolution from $t = 0$ to t_1.

To get rid of the common phase between $A_2(t_1)$ and $B_2(t_1)$, we multiply by $A_2^*(t_1)$ in Eqs. (26) and (28), and noting that $|A_1(-\infty)| = 1$ [which is easy to see from Eq. (12) with the initial condition $d_1(-\infty) = 1$]. We find

$$A_2(t_1) = 1, \tag{29}$$

$$B_2(t_1) = \sqrt{P_{LZ}} \exp[-3i\pi/4] \exp[2i\psi], \tag{30}$$

with

$$\psi = \frac{1}{\hbar} \int_0^{t_1} dt \left(V_1^d(t) - V_2^d(t)\right). \tag{31}$$

We now apply the LZ approximation to Eq. (24) with $V_2^d(t) - V_1^d(t) = v_0 F_{12}(t - 2t_1)$, so that

$$B_2(t_2) \simeq B_2(t_1) - i/\hbar V_c A_2(t_1) \int_{t_1}^{t_2} dt \exp\left[i/\hbar (v_0 F_{12}(t - 2t_1)^2/2)\right], \tag{32}$$

$$A_2(t_2) \simeq A_2(t_1). \tag{33}$$

Changing variables to $t'' = t - 2t_1$ and evaluating the Gaussian integral in Eq. (32) from -∞ to ∞ as before leads to

$$B_2(t_2) = B_2(t_1) + A_2(t_1)\sqrt{P_{LZ}} \exp[-i\pi/4]. \tag{34}$$

Substituting Eqs. (29) and (30) in Eq. (34) gives

$$B_2(t_2) = \sqrt{P_{LZ}} \exp[-i\pi/4] \{\exp[-i\pi/2] \exp[2i\psi] + 1\}. \tag{35}$$

The fraction of trajectories that switch diabat through this crossing is thus

$$|B_2(t_2)|^2 - |B_2(t_1)|^2 = 4P_{LZ} \cos^2(\psi - \pi/4) - P_{LZ}. \tag{36}$$

Equation (36) should hold as long as $|B_2(t_2)|^2 - |B_2(t_1)|^2 > 0$, i.e., $4\cos^2(\psi - \pi/4) > 1$. If this condition does not hold, then no diabatic transition will take place during this second crossing.

3. Crossing 3

For the final crossing (Fig. 2(c)), provided that A-FSSH collapses the amplitudes at the (x_2, t_2) turning point (as mentioned above), we note that all trajectories will have diabatic coefficient $d_2 = 1$. Thus, each and every trajectory on the upper surface again reverses itself and each trajectory will (if we ignore events with probability P_{LZ}^2) transmit on the same diabat (as shown by the blue arrow in Fig. 2(c)). Adding up the contributions from these two crossings leads to the final result given in Eq. (9).

IV. COMPUTATIONAL DETAILS

We now give a few computational details for our A-FSSH calculations and the exact quantum-mechanical calculations.

A. A-FSSH

For A-FSSH dynamics, the velocity-Verlet scheme is used for the evolution of the classical trajectory, and fourth order Runge-Kutta method is used to evolve the quantum amplitudes and the moments $\delta\mathbf{x}$, $\delta\mathbf{P}$ [see Appendix A].[41] An integration time step of 0.01 fs is used for all calculations. An average over 50 000 trajectories is taken for statistical averaging.

In our analysis below, sometimes it will be useful to compute an average transmission coefficient as[42]

$$\kappa_{ave} = \frac{\int dE \kappa(E) e^{-E^2/2\sigma_E^2}}{\int dE e^{-E^2/2\sigma_E^2}}. \tag{37}$$

We set the width $\sigma_E = 0.005$ a.u.[43] Equation (37) corresponds to the transmission of a wavepacket (rather than a plane wave).

B. Exact

Exact scattering results are obtained by solving for exact (multichannel) scattering state on a grid with spacing dx = 0.01 a.u. and a 5-stencil finite difference matrix for kinetic energy. The algorithm is described in detail in Ref. 44.

V. RESULTS

A. Diabatic regime

We first show results in the diabatic regime, $C = 0.0005$ a.u. in Fig. 3. Our results are compared against exact scattering computations. Both exact and the semiclassical results exhibit

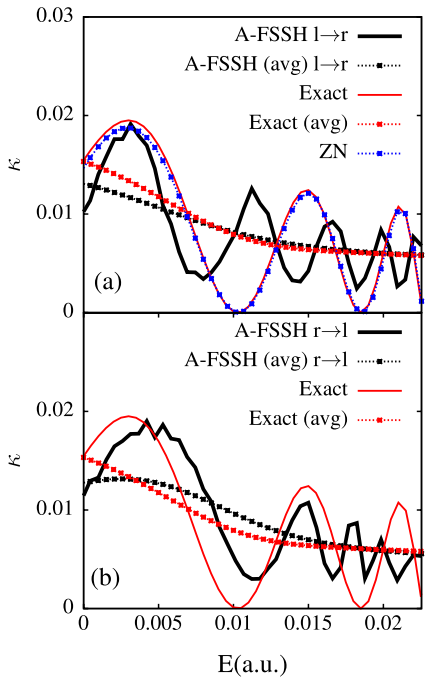

FIG. 3. (a) Forward and (b) backward transmission coefficients κ as a function of the energy of the system with $B_2 = 2.4$ and $C = 0.0005$. C is small enough such that this crossing is near the diabatic limit. The results are computed using A-FSSH simulations, exact scattering calculations and the ZN theory (which is nearly exact). Both the forward and the backward averaged transmission coefficients agree reasonably well with the averaged exact results, though the oscillations of the A-FSSH results occur at incorrect frequencies.

non-monotonic trends with energy, although with different frequencies. The oscillations in the transmission coefficient $\kappa(E)$ as a function of energy are the result of wavepacket interference and coherence in the crossing region. The averaged A-FSSH results [see Eq. (37)] agree reasonably well with the averaged exact results. However, the oscillations in the A-FSSH transmission coefficients as a function of energy E occur at incorrect frequencies as compared with exact results. This disagreement can be understood by comparing Eq. (9) with ZN theory in the diabatic regime. In this regime, according to ZN, the transmission coefficient is[29]

$$\kappa_{ZN} = 4P_{LZ}\cos^2(\sigma - \pi/4), \tag{38}$$

where

$$\sigma = \frac{1}{\hbar}\int_{x_2}^{x_1} dx\sqrt{2m(E - V_2(x))} \tag{39}$$

is the action integral. Here, x_1 and x_2 are the classical turning points on the upper adiabat $V_2(x)$ at total energy E [see Fig. 2]. Equation (38) is plotted in Fig. 3(a) to convince the reader that κ_{ZN} matches very well with exact scattering theory results. Going back to A-FSSH, the phase ψ in Eq. (10) integrates the potential only towards the right side (for forward reaction), while the phase σ in Eq. (39) is symmetric about the crossing point. Interestingly, $B_1 = B_2$ is a special case where the oscillations in the exact results and the A-FSSH match well at low energies — this case is discussed in detail in Appendix B.

B. Adiabatic regime

Figure 4 shows results in the adiabatic regime, $C = 0.005$ a.u. As in the diabatic regime, there are oscillations in the transmission coefficient as a function of energy. In fact, compared with the diabatic regime, these oscillations are quite large and cannot be recovered with A-FSSH. Nevertheless, the average A-FSSH κ compares well with exact results at reasonably large energies where tunneling and frustrated hops are not important ($E > 0.01$ a.u.). The averaged left-to-right and the right-to-left transmission coefficients are very similar.

One word is now required regarding velocity reversal. In the very low energy regime ($E < 0.002$ a.u.), trajectories do not have enough energy to hop, and all attempted hops are forbidden. Thus, without any velocity reversal, the transmission coefficient would be always unity. With velocity reversal, however, A-FSSH results are improved and results are in better comparison with the exact results. We discuss the issue of frustrated hops in greater detail in Paper II.[11]

C. Decoherence

To clarify the role of decoherence, calculations were performed in the diabatic regime without any decoherence, marked as FSSH in Fig. 5. Interestingly, the FSSH results are reasonably close to the LZ transmission coefficient P_{LZ} and do not show any oscillations as a function of energy. This behavior can be explained intuitively as follows. At the first crossing, P_{LZ} fraction of trajectories are transmitted, and $1 - P_{LZ}$ hop to the upper adiabat (see Fig. 2(a)). In the absence of any decoherence, no trajectory on the upper adiabat switches

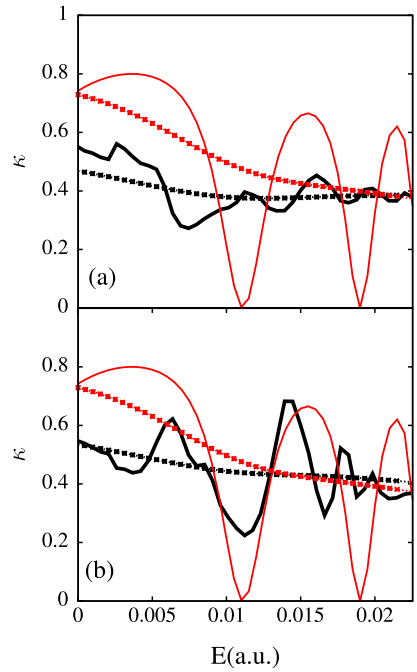

FIG. 4. Same as in Fig. 3 but with $C = 0.005$ a.u. C is now large enough such that the crossing is near adiabatic limit. The legend is the same as in Fig. 3. Exact results (shown red) and A-FSSH results (black) have very different oscillatory structures. Below $E = 0.002$ a.u., all hops are forbidden. However, for reasonably large energies (where tunneling and frustrated hops are not important), the averaged A-FSSH transmission coefficients (both forward and backward) compare well with averaged exact data.

diabats. As a consequence, ignoring events with probability P_{LZ}^2, these trajectories are all reflected. In effect, this implies that FSSH transmission coefficient is entirely κ missing all dynamical effects from the upper adiabat.

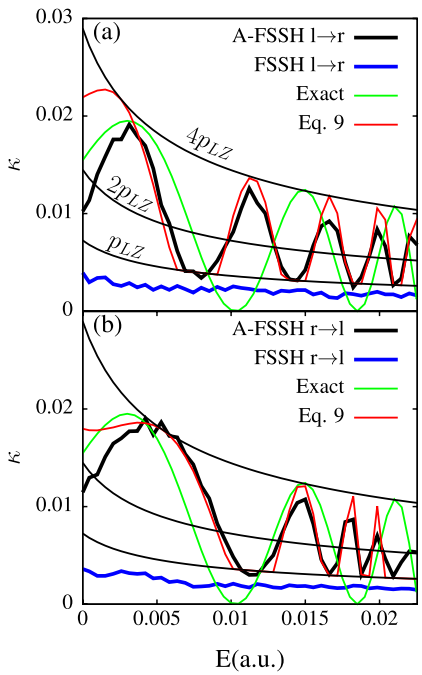

FIG. 5. Comparison of the (a) forward and (b) backward A-FSSH and FSSH transmission coefficients (κ) with Eq. (9) for $B_2 = 2.4$ a.u. and $C = 0.0005$ a.u. The A-FSSH simulation results match well with those of Eq. (9), recovering some of the oscillations in transmission, while the FSSH results underestimate the transmission coefficients.

Next, consider A-FSSH trajectories which predict decoherence mostly at the x_2 turning point (see Fig. 2). Numerical evidence for this assumption is provided in Appendix C. In this case, surface hopping results show some oscillations and can vary between P_{LZ} and $4P_{LZ}$ as a function of energy according to Eq. (9). Further, as also shown in Appendix C, the contribution to κ from the trajectories that never hop (see Fig. 2(a)) is roughly P_{LZ} (as was obtained from FSSH), and the rest of the contribution nearly comes from trajectories with 3 recrossings. On average, the transmission coefficient is not far from $2P_{LZ}$, which is consistent with Fermi's golden rule and Marcus theory;[45] the factor 2 appears since there are two chances to switch diabats for every crossing event.

Finally, if the trajectories decohere at both the turning points, or whenever the trajectory leaves the strong nonadiabatic coupling region (not shown), we mention that surface hopping transmission is very close to $2P_{LZ}$ (just like the averaged A-FSSH). However, in this case, there are no oscillations at all in the transmission coefficient (just like for FSSH).

Before concluding, we want to mention a few more words about A-FSSH and time-reversibility. According to ZN theory, clearly transmission coefficients are time-reversible: the forward and backward σ in Eq. (39) are identical. However, for A-FSSH, this time-reversibility does not hold. Using Eq. (9) above, it is straightforward to see why. For time-reversible dynamics (that obey microscopic reversibility), we must insist that

$$\int_0^{t_1} dt \left(V_1^d(t) - V_2^d(t)\right) = \int_0^{t_2} dt \left(V_2^d(t) - V_1^d(t)\right), \quad (40)$$

which does not hold in general. Nevertheless, we have found that the thermal average in either directions is $2P_{LZ}$ and, as such, a thermal rate constant should obey detailed balance approximately[46] (consistent with the population results of Schmidt, Parandekar, and Tully).[25] This statement about rate constants will be explored in detail in Paper II.[11]

D. Curve crossing initialization

Having shown that direct A-FSSH gives reasonably good transmission factors, we now compare scattering results that are initiated asymptotically with those initiated at the curve crossing. Results are shown in Figure 6. The agreement between the two different forward $\kappa(E)$'s (and also between the two different backward $\kappa(E)$'s) is very encouraging and would appear to justify our assumption of running backward dynamics purely on the ground surface. (Note that, in Fig. 6, we provide data only in the diabatic regime; we also obtain excellent agreement in the adiabatic regime.)

Finally, the last and the most important question we must address is this: Can accurate calculations still be achieved if the location of the curve crossing is not known? To answer this question, we vary the starting point in the algorithm presented in Sec. III B (step 1) above and calculate κ at energy E = 0.0155 a.u. The results are shown in Fig. 7, where the x-axis corresponds to the starting position relative to $x^\ddagger$ in Fig. 1. Notice that we find a broad region where κ is approximately constant. In fact, so long as we choose the initial point to be between the classical turning points x_1 and x_2 on the upper adiabat, we should find a reasonable κ. To understand the extent of this constant region, and our margin of error in choosing a curve crossing location, consider the forward computation. If the initial point is chosen with $x > x_1$, a hop at this point will be

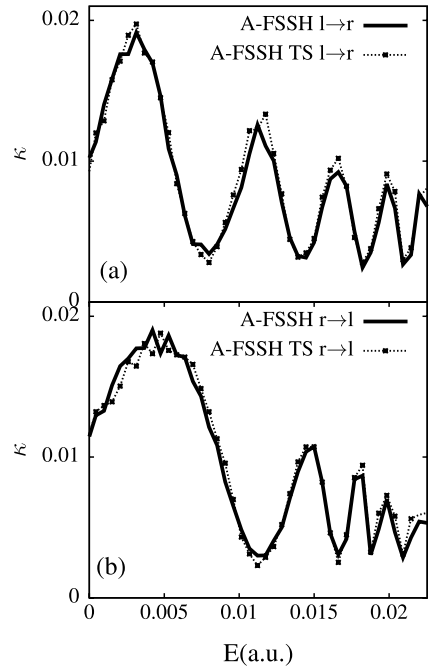

FIG. 6. Comparison of the (a) forward and (b) backward A-FSSH transmission coefficients (κ) obtained by initiating at $x = -2$ Å (solid line) and at the curve crossing point $x^\ddagger$ from Fig. 1 (dotted line). Note the excellent agreement between the direct calculations and the TST calculations.

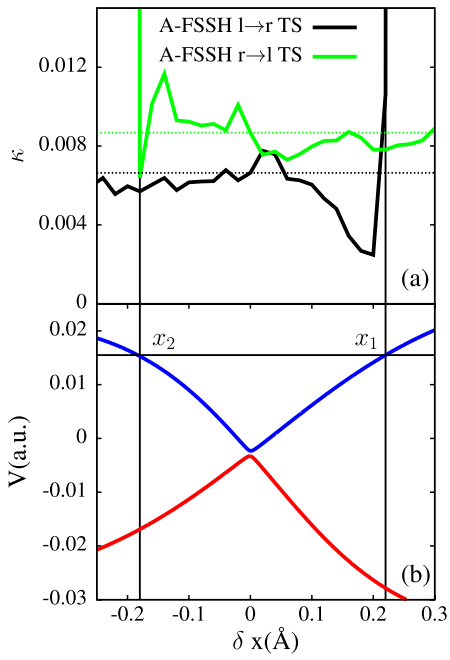

FIG. 7. (a) The A-FSSH results obtained by initiating at $x_{\text{init}} = x^\ddagger + \delta x$, where $x^\ddagger$ is the position of curve crossing. The forward rate is shown in black, while the backward rate is shown in green. The dotted line marks the result at $\delta x = 0$ as a guide to the eye. (b) The adiabatic potential energy surfaces as a function of δx. The classical turning points x_1 and x_2 are marked at the energy of 0.0155 a.u. Note that one can roughly recover the correct transmission coefficient as long as the starting point x_{init} lies between these turning points.

frustrated. This leads to a situation where all of the trajectories are getting initiated on the ground surface (see step 3 of the algorithm in Sec. III B), even though the quantum amplitude of the ground surface is small ($|c_1|^2 \sim P_{LZ}$). These trajectories will then continue forward to the product well giving $\kappa \sim 1$ (except for a small fraction of trajectories that experience a forbidden hop during the forward evolution, reversing their velocities and turning back towards the reactant side).

VI. CONCLUSIONS

We have provided an in-depth investigation of transmission coefficients as computed using the A-FSSH algorithm in the low energy regime. In general, we can show semiclassically that surface hopping can recover the correct oscillations in the transmission function (as a function of energy) only by chance. However, provided that decoherence is treated properly (e.g., with A-FSSH), surface hopping recovers, on average, the correct transmission ratio. Furthermore, on average, microscopic reversibility holds approximately in both the adiabatic and diabatic regimes.

Looking forward, our results in Fig. 6 should be very important for practical evaluations of thermal rate constants in the condensed phase. Here, we have shown that back-propagation solely on the ground adiabat can, at least sometimes, be sufficient for initializing quantum amplitudes at the curve-crossing—both in terms of accuracy and numerical stability. This finding agrees with the results of Hammes-Schiffer and Tully[12] even though we are using a simpler approximation. In Paper II, we will explore the Marcus problem and non-adiabatic transition state theory in the condensed phase using the present approach.[11]

ACKNOWLEDGMENTS

This material is based upon work supported by the (U.S.) Air Force Office of Scientific Research (USAFOSR) PECASE award under AFOSR Grant No. FA9950-13-1-0157. J.E.S. acknowledges a Cottrell Research Scholar Fellowship and a David and Lucille Packard Fellowship.

APPENDIX A: A-FSSH ALGORITHM STEP-BY-STEP

For completeness, we here describe the basic steps of an A-FSSH calculation to compute the forward transmission coefficient directly. We closely follow the algorithm presented in Ref. 18, with two differences: (i) a simplified treatment of the moments adjustment after a successful hop and (ii) the reversal of velocity on encountering forbidden hops, both of which are described in step 4. The algorithm is given for the Hamiltonian defined in Eqs. (1)-(3), with the nuclear position and momentum given by x and P, respectively. The quantum amplitudes are denoted by c_j, the non-adiabatic coupling vector as d_{ij}, and the moments of the positions and momentum as δx_{jk} and δP_{jk}, respectively.

1. For a given energy E, initialize the position $x = -2$ Å, the momentum $P = \sqrt{2m(E+A)}$, and the quantum amplitudes $c_1 = 1$ and $c_2 = 0$. Set the moments $\delta x_{jk} = 0$ and $\delta P_{jk} = 0$.
2. For the time step dt, evolve
   - the classical dynamics using
   $$\dot{x} = \frac{P}{m}, \tag{A1}$$
   $$\dot{P} = -\frac{\partial V_i}{\partial x}, \tag{A2}$$
   where i labels the active potential energy surface and V_i the corresponding adiabatic potential energy surface,
   - the quantum dynamics using
   $$i\hbar\begin{pmatrix}\dot{c_1}\\ \dot{c_2}\end{pmatrix} = \begin{pmatrix}V_1 & -i\hbar(P/m)d_{12}\\ i\hbar(P/m)d_{12} & V_2\end{pmatrix}\begin{pmatrix}c_1\\ c_2\end{pmatrix}, \tag{A3}$$
   - the moments as
   $$\delta\dot{x}_{jk} = T^x_{jk} - T^x_{ii}\delta_{jk}, \tag{A4}$$
   $$\delta\dot{P}_{jk} = T^P_{jk} - T^P_{ii}\delta_{jk}, \tag{A5}$$
   with
   $$T^x_{jk} \equiv -\frac{i}{\hbar}[\hat{V},\delta\hat{x}]_{jk} + \frac{\delta P_{jk}}{m} - \frac{P_{SH}}{m}[\hat{d},\delta\hat{x}]_{jk}, \tag{A6}$$
   $$T^P_{jk} \equiv -\frac{i}{\hbar}[\hat{V},\delta\hat{P}]_{jk} + \frac{1}{2}\left(\delta\hat{F}\hat{\sigma} + \hat{\sigma}\delta\hat{F}\right)_{jk} - \frac{P_{SH}}{m}[\hat{d},\delta\hat{P}]_{jk}, \tag{A7}$$
   where i stands for the active surface, with momentum P_{SH}. $\hat{V}$, $\hat{F}$, and $\hat{d}$ are the matrices of the potential energy surfaces, forces, and the non-adiabatic coupling, respectively. The matrix of force differences is defined as $\delta\hat{F} = \hat{F} - F_{SH}\hat{I}$, where F_{SH} is the force on the active surface and $\hat{I}$ is the identity matrix. We have also defined $\hat{\sigma}_{jk} = c_j c_k^*$.
3. Compute the hopping probability as
   $$\gamma^{i\to j}_{hop} = -\frac{2P}{m}\frac{\mathrm{Re}(d_{ji}c_i c_j^*)}{|c_i|^2}dt. \tag{A8}$$
   If this probability is less than zero, it is set to 0. For a pseudo-random number ζ, if $\zeta < \gamma^{i\to j}_{hop}$, proceed to step 4, otherwise go to step 5.
4. When the hop from state i to j takes place, a new momentum P_n is computed to conserve energy as
   $$P_n = \pm\sqrt{2m\left(\frac{1}{2m}P^2 + V_i - V_j\right)}, \tag{A9}$$
   where P is the current momentum. In the above equation, positive sign is chosen for $P > 0$ and negative sign for $P < 0$. If P_n comes out to be complex, that is, there is not enough energy to hop, the hop is forbidden. Following the works of Truhlar,[35] we reverse the momentum for these forbidden hops if (i) $F_1F_2 < 0$ and (ii) $PF_2 < 0$, where $F_1(F_2)$ is the force on the adiabat 1 (2). The importance of velocity reversal is discussed in Paper II.[11] If the hop is allowed, all the position and momentum moments are set to 0.
5. Compute the probability to collapse the amplitudes for the state $n \neq i$ (where i is the active surface) as
   $$\gamma^{collapse}_n = dt\left(\frac{(F_{nn} - F_{ii})\delta x_{nn}}{2\hbar} - \frac{2|F_{in}\delta x_{nn}|}{\hbar}\right). \tag{A10}$$

Also compute the probability to reset the moments as

$$\gamma_n^{reset} = -dt\left(\frac{(F_{nn} - F_{ii})\delta x_{nn}}{2\hbar}\right). \tag{A11}$$

Compute a random number ζ. If $\zeta < \gamma_n^{reset}$, then set

$$\delta x_{jn} = \delta x_{nj} = 0, \text{ for all j and} \tag{A12}$$
$$\delta P_{jn} = \delta P_{nj} = 0, \text{ for all j.} \tag{A13}$$

If $\zeta < \gamma_n^{collapse}$, then in addition to the above resetting of the moments, we also set $c_j = \delta_{ij}$.

6. Iterate all trajectories until $|x| > 2$ Å. Compute the transmission coefficient as the ratio of the trajectories terminated for $x > 2$ Å to the total number of trajectories run.

APPENDIX B: EQUAL DIABATIC SLOPES $B_1 = B_2$

In the body of the manuscript above, we analyzed the general case $B_1 \neq B_2$ in Eq. (2). The case $B_1 = B_2$ is special. Results are shown in Fig. 8. In contrast to Figs. 3 and 4, according to Fig. 8, A-FSSH now agrees with the exact results including the oscillation in κ as a function of energy. This agreement is entirely an artifact of the fact that the diabatic slopes are same at the curve crossing. In this case, when $B_1 = B_2$, assuming the diabats can be replaced with straight lines from x_1 to x_2 (in Fig. 2), one can easily show that $\psi = \sigma$ (see below). Because the approximation of linear diabats holds well in the low energy regime, exact and A-FSSH results agree very well. In the high energy regime, however, differences begin to appear because ψ and σ are no longer approximately equal.

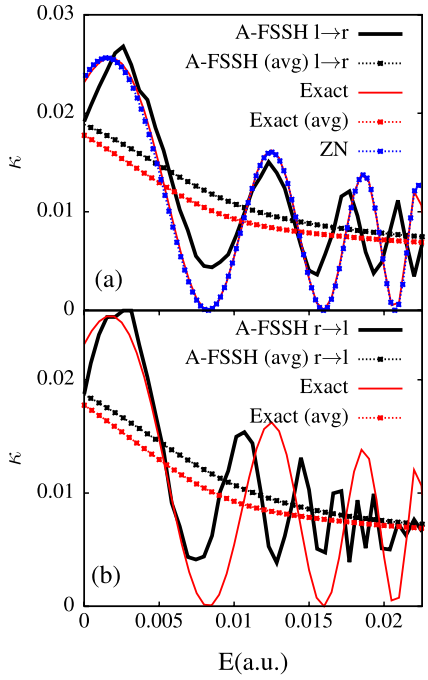

FIG. 8. Same as in Fig. 3 but with $B_2 = 1.6$ a.u. We now find a coincidental agreement between the oscillations of the A-FSSH and exact results, particularly in the low energy regime. This is an artifact choosing $B_1 = B_2$ in Eqs. (1) and (2).

Let us now show that $\psi = \sigma$ given that (a) $B_1 = B_2 \equiv B$ and (b) both diabats can be replaced with straight lines

$$V_1^d = Bx, \tag{B1}$$
$$V_2^d = -Bx. \tag{B2}$$

Consider Eq. (39),

$$\sigma = \frac{1}{\hbar}\int_{x_2}^{x_1} dx\sqrt{2m(E - V_2(x))}, \tag{B3}$$

where $V_2(x)$ is the upper adiabatic surface. If we assume the diabatic limit, such that $V_1^d(x) = V_2(x)$ for $x > x^{\ddagger}$ and use the fact that $B_1 = B_2$, we find

$$\sigma = \frac{2}{\hbar}\int_0^{x_1} dx\sqrt{2m(E - V_1^d(x))}. \tag{B4}$$

Substituting Eq. (B1) into Eq. (B4) and recognizing that $E = Bx_1$ leads to

$$\sigma = \frac{2}{\hbar}\sqrt{2mB}\int_0^{x_1} dx\sqrt{x_1 - x} \tag{B5}$$
$$= \frac{4}{3\hbar}\sqrt{2mB}x_1\sqrt{x_1}. \tag{B6}$$

Now, we evaluate Eq. (10) as

$$\psi = \frac{1}{\hbar}\int_0^{t_1} dt(V_1^d(t) - V_2^d(t)) \tag{B7}$$
$$= \frac{1}{\hbar}\int_0^{x_1} dx\frac{(V_1^d(x) - V_2^d(x))}{\sqrt{2/m(E - V_1^d(x))}}. \tag{B8}$$

Here, we have switched variables from t to x and used energy conservation $v = \sqrt{2/m(E - V_1^d)}$. As above, we substitute Eqs. (B1) and (B2) and use $E = Bx_1$, leading to

$$\psi = \frac{1}{\hbar}\sqrt{2mB}\int_0^{x_1} dx\frac{x}{\sqrt{x_1 - x}} \tag{B9}$$
$$= \frac{4}{3\hbar}\sqrt{2mB}x_1\sqrt{x_1}. \tag{B10}$$

Comparing Eqs. (B6) and (B10) proves the desired result: $\psi = \sigma$.

APPENDIX C: DECOHERENCE AND RECROSSINGS STATISTICS

In Sec. III C, we assumed that, for A-FSSH, all decoherence events occur at the x_2 turning point (for the forward reaction; see Fig. 2). This assumption is crucial to explain the oscillations observed in the A-FSSH trajectories. Here, we provide numerical support for this assumption. Further, we also provide statistics on the contribution to the transmission coefficients from (a) direct transmission [Fig. 2(a)], (b) 3 recrossings [Figs. 2(b) and 2(c)], and (c) multiple recrossings (not considered in Fig. 2). We will consider the case $B_2 = 2.4$, and $C = 0.0005$. Statistics are obtained by averaging over 50 equally spaced energy values ranging from 0.0023 a.u. to 0.022 a.u. For each energy value, 50 000 trajectories are used.

In Fig. 9, we make a histogram of decoherence events occurring on the upper adiabat for reactive trajectories as a function of position. Roughly 92% of the collapse events occur to the left of the curve crossing point (and towards the x_2

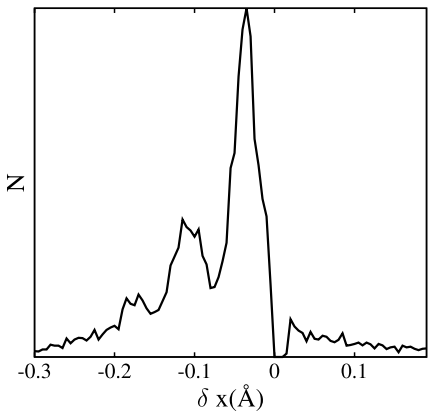

FIG. 9. Normalized histogram of collapse events on the upper adiabat for reactive trajectories. Most of the collapse (92%) occurs to the left of the curve-crossing ($\delta x = 0$). Here, $B_2 = 2.4$ and $C = 0.0005$ (see Eqs. (1)-(3)). Statistics are obtained using 50 000 trajectories for 50 equally spaced energy values ranging from 0.0023 a.u. to 0.022 a.u. over a range of positions from $\delta x = -0.3$ Å to 0.2 Å with bin spacing 0.005 Å.

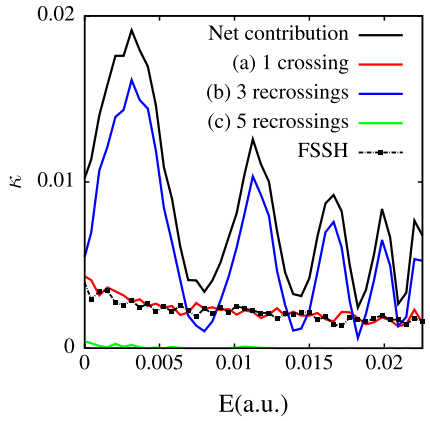

FIG. 10. Contribution to the total transmission coefficient from trajectories with different recrossings computed using A-FSSH calculations. The FSSH results are also shown, which compare very well with the single crossing contribution to the A-FSSH results. The potential parameters are $B_2 = 2.4$ and $C = 0.0005$.

crossing point). We note here that the collapse need not occur at exactly x_2 for the semiclassical result Eq. (9) to hold — we require only that the collapse occur left of the curve-crossing.

Next, in Fig. 10 we consider the contribution of various categories of A-FSSH trajectories to the overall transmission. FSSH results are also shown in this figure. Directly transmitting A-FSSH trajectories [case (a)] agree with FSSH trajectories. In-fact, 98% of the contribution to the FSSH contributions come from direct transmission. For A-FSSH, the net transmission is given to a very good approximation (in this diabatic limit) by the sum of direct transmission and 3 recrossings [case (b)]. On average the contribution from case (a) and (b) are roughly equal for a total average transmission of $2P_{LZ}$. Trajectories with more than 3 recrossings contribute only 0.6% to the total A-FSSSH transmission coefficient.

[1]J. C. Tully, J. Chem. Phys. **93**, 1061 (1990).
[2]U. Müller and G. Stock, J. Chem. Phys. **107**, 6230 (1997).
[3]S. Hammes-Schiffer and J. C. Tully, J. Chem. Phys. **101**, 4657 (1994).
[4]M. Barbatti, WIREs: Comput. Mol. Sci. **1**, 620 (2011).
[5]R. Marcus, Annu. Rev. Phys. Chem. **15**, 155 (1964).
[6]J. T. Hynes, Annu. Rev. Phys. Chem. **36**, 573 (1985).
[7]A. Warshel and J.-K. Hwang, J. Chem. Phys. **84**, 4938 (1986).
[8]B. J. Berne, M. Borkovec, and J. E. Straub, J. Phys. Chem. **92**, 3711 (1988).
[9]P. Hänggi, P. Talkner, and M. Borkovec, Rev. Mod. Phys. **62**, 251 (1990).
[10]E. Pollak and P. Talkner, Chaos **15**, 026116 (2005).
[11]A. Jain and J. Subotnik, J. Chem. Phys. **143**, 134107 (2015).
[12]S. Hammes-Schiffer and J. C. Tully, J. Chem. Phys. **103**, 8528 (1995).
[13]J. E. Subotnik and Y. M. Rhee, J. Phys. Chem. A **119**, 990 (2015).
[14]B. J. Schwartz, E. R. Bittner, O. V. Prezhdo, and P. J. Rossky, J. Chem. Phys. **104**, 5942 (1996).
[15]M. J. Bedard-Hearn, R. E. Larsen, and B. J. Schwartz, J. Chem. Phys. **123**, 234106 (2005).
[16]G. Granucci, M. Persico, and A. Zoccante, J. Chem. Phys. **133**, 134111 (2010).
[17]B. R. Landry and J. E. Subotnik, J. Chem. Phys. **135**, 191101 (2011).
[18]B. R. Landry and J. E. Subotnik, J. Chem. Phys. **137**, 22A513 (2012).
[19]J. E. Subotnik, W. Ouyang, and B. R. Landry, J. Chem. Phys. **139**, 214107 (2013).
[20]M. F. Herman, J. Chem. Phys. **76**, 2949 (1982).
[21]M. F. Herman, J. Phys. Chem. A **109**, 9196 (2005).
[22]M. F. Herman and M. P. Moody, J. Chem. Phys. **122**, 094104 (2005).
[23]M. F. Herman, Chem. Phys. **433**, 12 (2014).
[24]R. E. Cline and P. G. Wolynes, J. Chem. Phys. **86**, 3836 (1987).
[25]J. R. Schmidt, P. V. Parandekar, and J. C. Tully, J. Chem. Phys. **129**, 044104 (2008).
[26]M. C. Sherman and S. A. Corcelli, J. Chem. Phys. **142**, 024110 (2015).
[27]C. Zener, Proc. R. Soc. A **137**, 696 (1932).
[28]C. Wittig, J. Phys. Chem. B **109**, 8428 (2005).
[29]C. Zhu and H. Nakamura, J. Chem. Phys. **101**, 10630 (1994).
[30]C. Zhu and H. Nakamura, J. Chem. Phys. **102**, 7448 (1995).
[31]C. Zhu, K. Nobusada, and H. Nakamura, J. Chem. Phys. **115**, 3031 (2001).
[32]C. Zhu, H. Kamisaka, and H. Nakamura, J. Chem. Phys. **116**, 3234 (2002).
[33]P. Oloyede, G. Milnikov, and H. Nakamura, J. Chem. Phys. **124**, 144110 (2006).
[34]A. W. Jasper, J. Phys. Chem. A **119**, 7339 (2015).
[35]A. W. Jasper and D. G. Truhlar, Chem. Phys. Lett. **369**, 60 (2003).
[36]S. Y. Kim and S. Hammes-Schiffer, J. Chem. Phys. **124**, 244102 (2006).
[37]If coherent, these crossing events cannot be treated with A-FSSH, and if incoherent, these crossing events should have no consequence.
[38]D. M. Kernan, G. Ciccotti, and R. Kapral, J. Phys. Chem. B **112**, 424 (2008).
[39]B. R. Landry and J. E. Subotnik, J. Chem. Phys. **142**, 104102 (2015).
[40]W. Xie, S. Bai, L. Zhu, and Q. Shi, J. Phys. Chem. A **117**, 6196 (2013).
[41]M. P. Allen and D. J. Tildesley, *Computer Simulation of Liquids* (Clarendon Press, New York, NY, USA, 1989).
[42]We use a Gaussian in energy (rather than momentum space) for simplicity (e.g., to avoid square roots).
[43]There is one nuance here. When evaluating the integral in Eq. (37) numerically, if the support of the integral extends over the edge of the integration domain, we cut off the integral at that edge (and renormalize our results accordingly).
[44]W. Ouyang, W. Dou, and J. E. Subotnik, J. Chem. Phys. **142**, 084109 (2015).
[45]M. D. Newton and N. Sutin, Annu. Rev. Phys. Chem. **35**, 437 (1984).
[46]Interestingly, for fully decoherent dynamics (where collapses occur on both sides of the crossing region), we expect the left to right and right to left transmission functions to agree nearly quantitatively (and with probability $2P_{LZ}$, respectively).